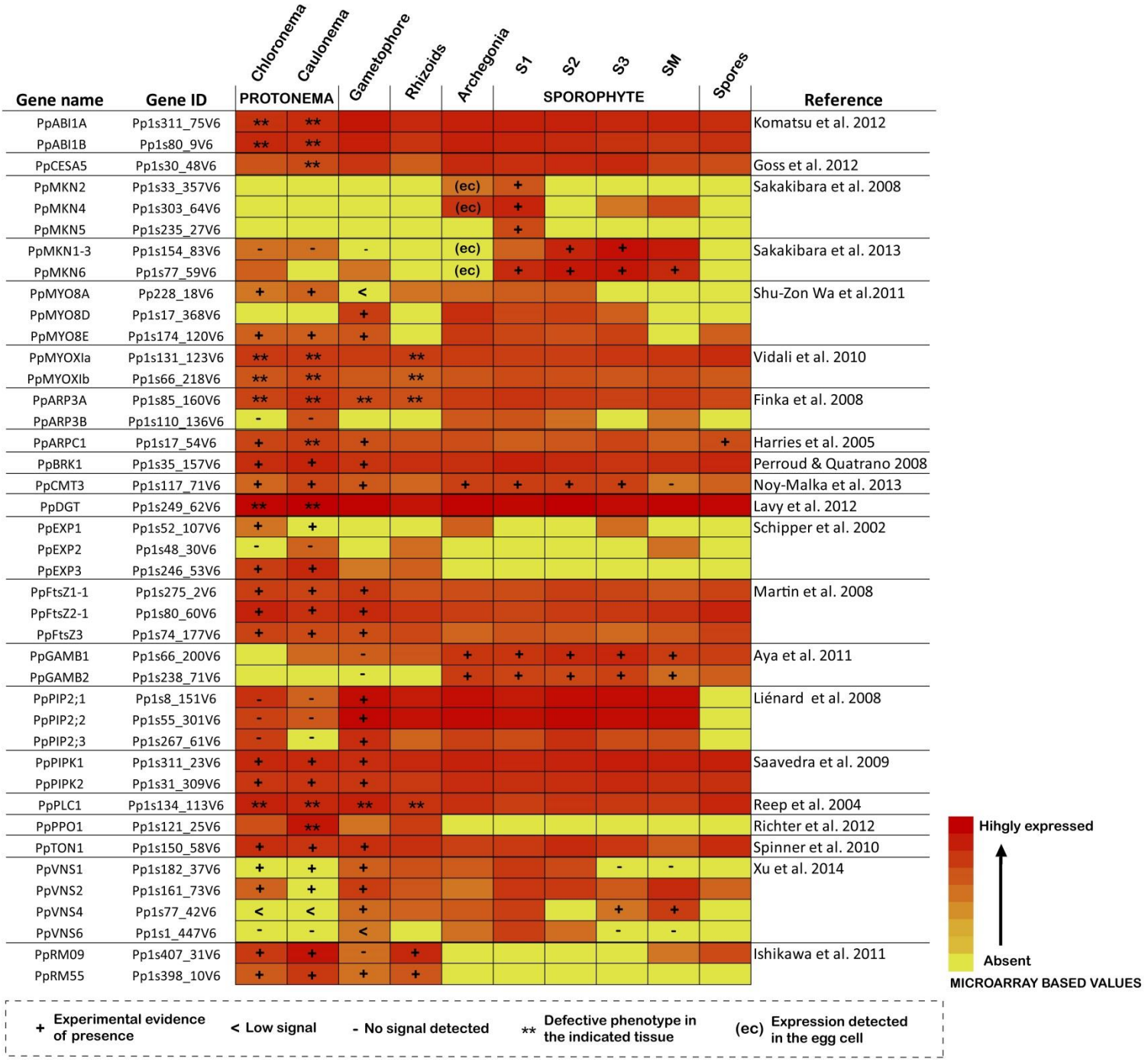

Supplemental Figure 1. Correlation of microarray expression values and published evidence. A bibliographical search was performed for published data on some of the genes present in our microarray with the purpose of correlating the expression values with experimental evidence. Gene name and gene identifiers are displayed on the left, while references in which such genes are mentioned are displayed on the right. In many cases several genes were evaluated in the same study. In the absence of tissue evidence (not studied or not shown), no symbol is displayed."+" means experimental evidence of presence, "<" indicates low GUS or GFP signal was detected by the authors, "-" no signal was detected, "**" indicates a defective phenotype was observed in corresponding tissues after gene K.O., and "(ec)" means detection in egg cell. Red represents high expression while yellow represents low expression values.

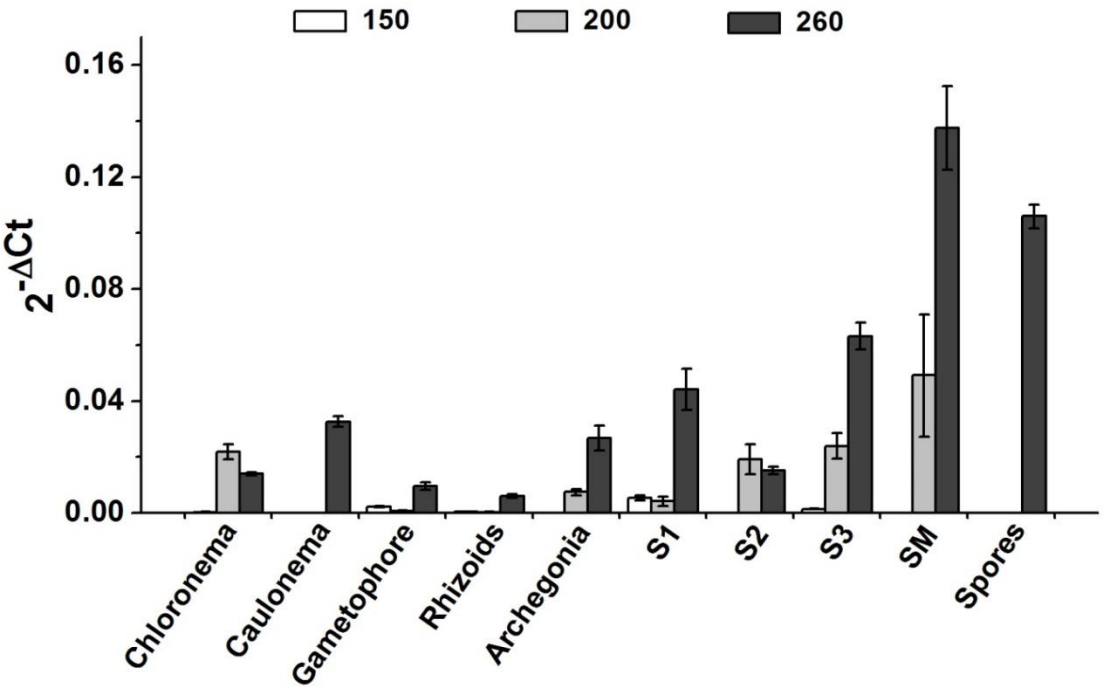

Supplemental Figure 2. Threshold determination for presence/absence detection calls. qRT-PCR experiments were conducted using excess cDNA synthetized for microarray hybridization from all *Physcomitrella* tissues. After a preliminary analysis we expected the detection threshold to be between the relative expression values of 150 to 260 as reported in the microarray data. Three genes per tissue with a relative expression values corresponding to 150, 200 and 260 were tested. From these, only the ones with a relative expression of 260 were always detected (amplified) by qRT-PCR.

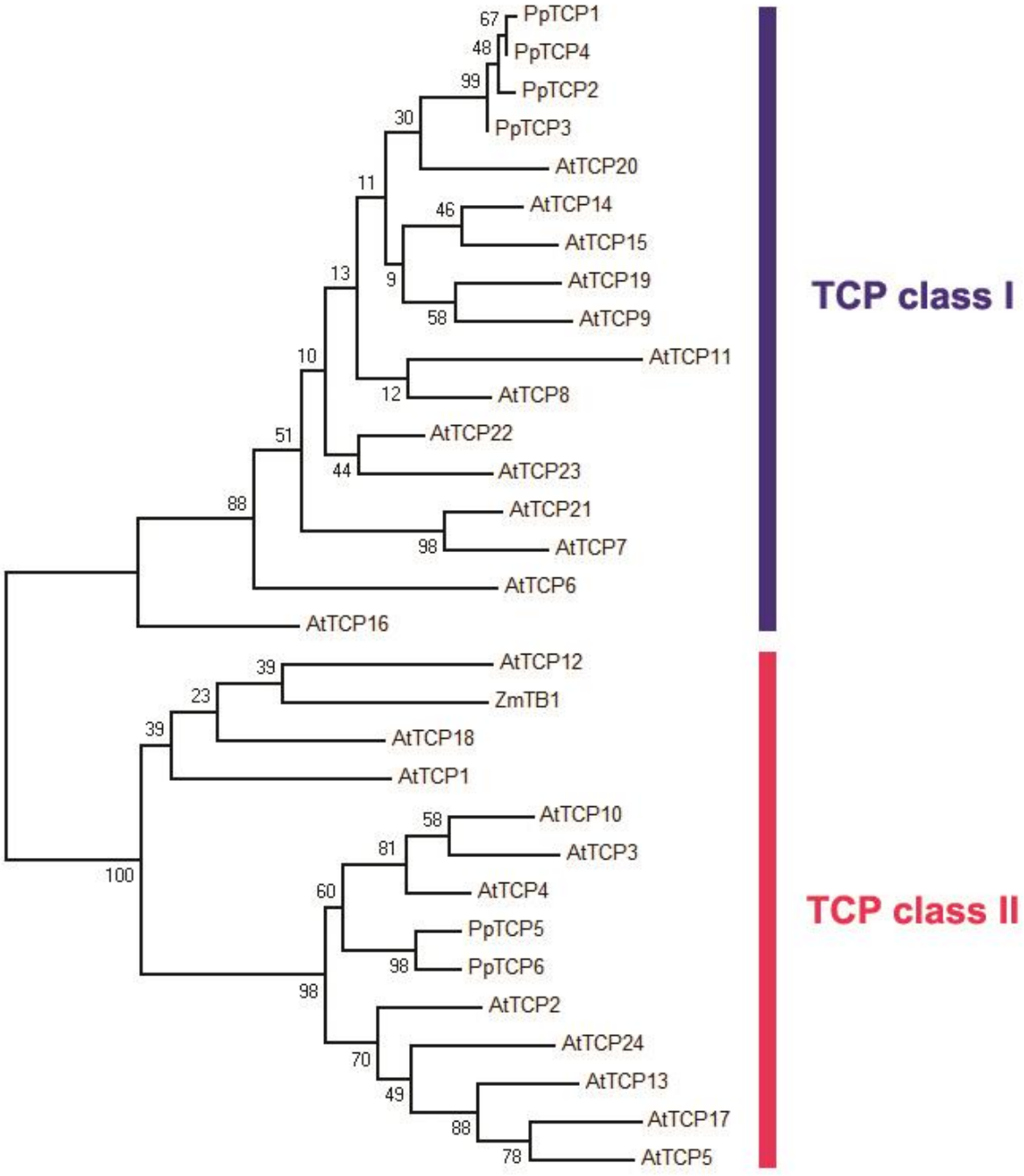

Supplemental Figure 3. Phylogenetic analysis of TCP genes. Phylogenetic tree constructed using maximum likelihood statistical method from aligned amino-acid sequences of TCP genes from *Arabidopsis thaliana (At), Physcomitrella patens (Pp)* and *Zea mays (Zm).* Bootstrap support values are shown at the nodes of the tree.

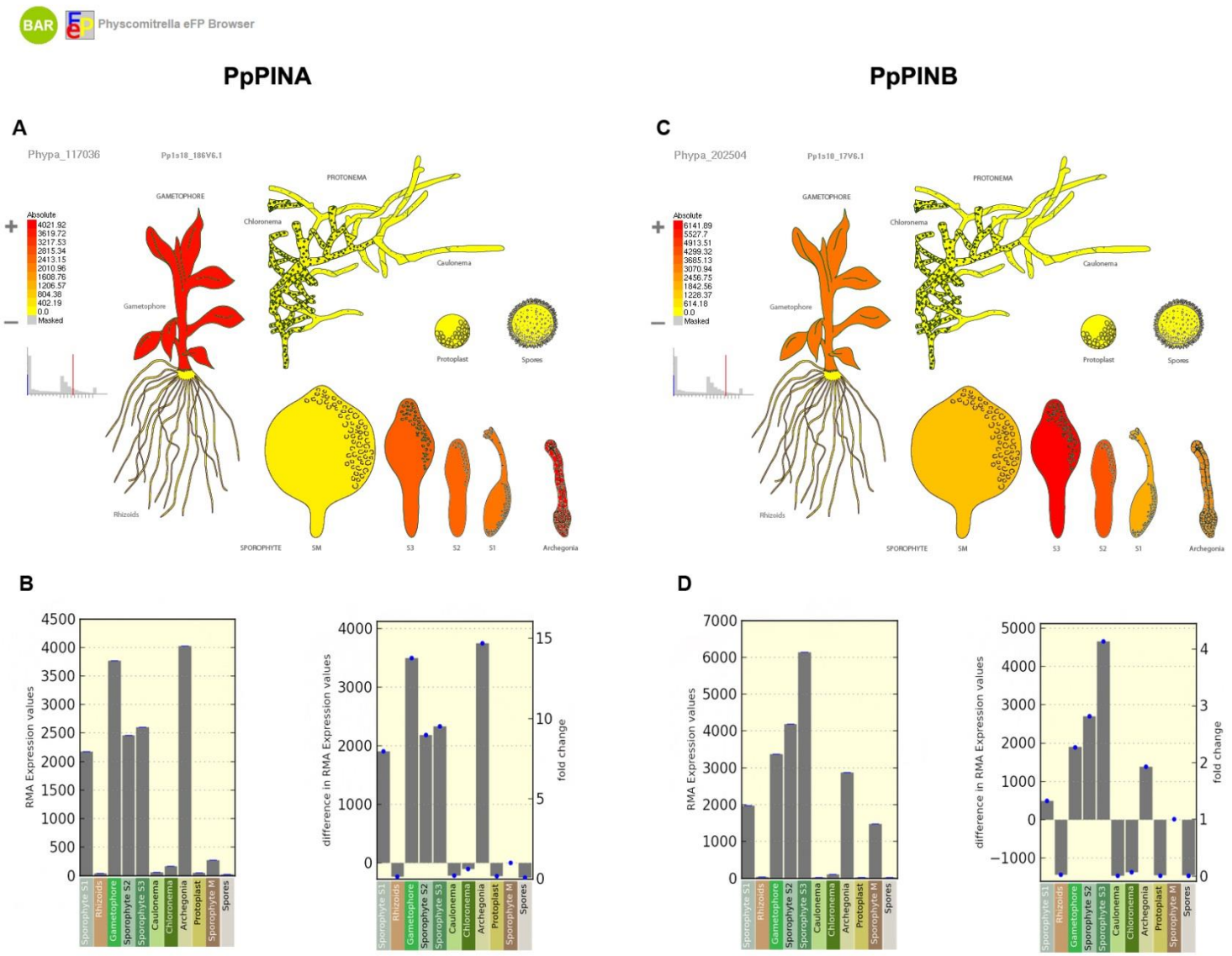

Supplemental Figure 4. PpPINA and PpPINB expression patterns as reported by the Physcomitrella eFP browser. A search was performed in the Physcomitrella eFP browser using the gene identifiers for PpPINA (Pp1s10_17V6.1) and PpPINB (Pp1s18_186V6.1). (a) Pictograph of *P. patens* tissues showing the expression profile of PpPINA in color code (red represents high expression while yellow represents low expression values). (b) Charts generated by the eFP browser showing PpPINA absolute (left) and relative (right) expression values for each tissue. (c) Pictograph of *P. patens* tissues showing the expression profile of PpPINB in color code. (d) Charts generated by the eFP browser showing PpPINB absolute (left) and relative (right) expression values for each tissue.

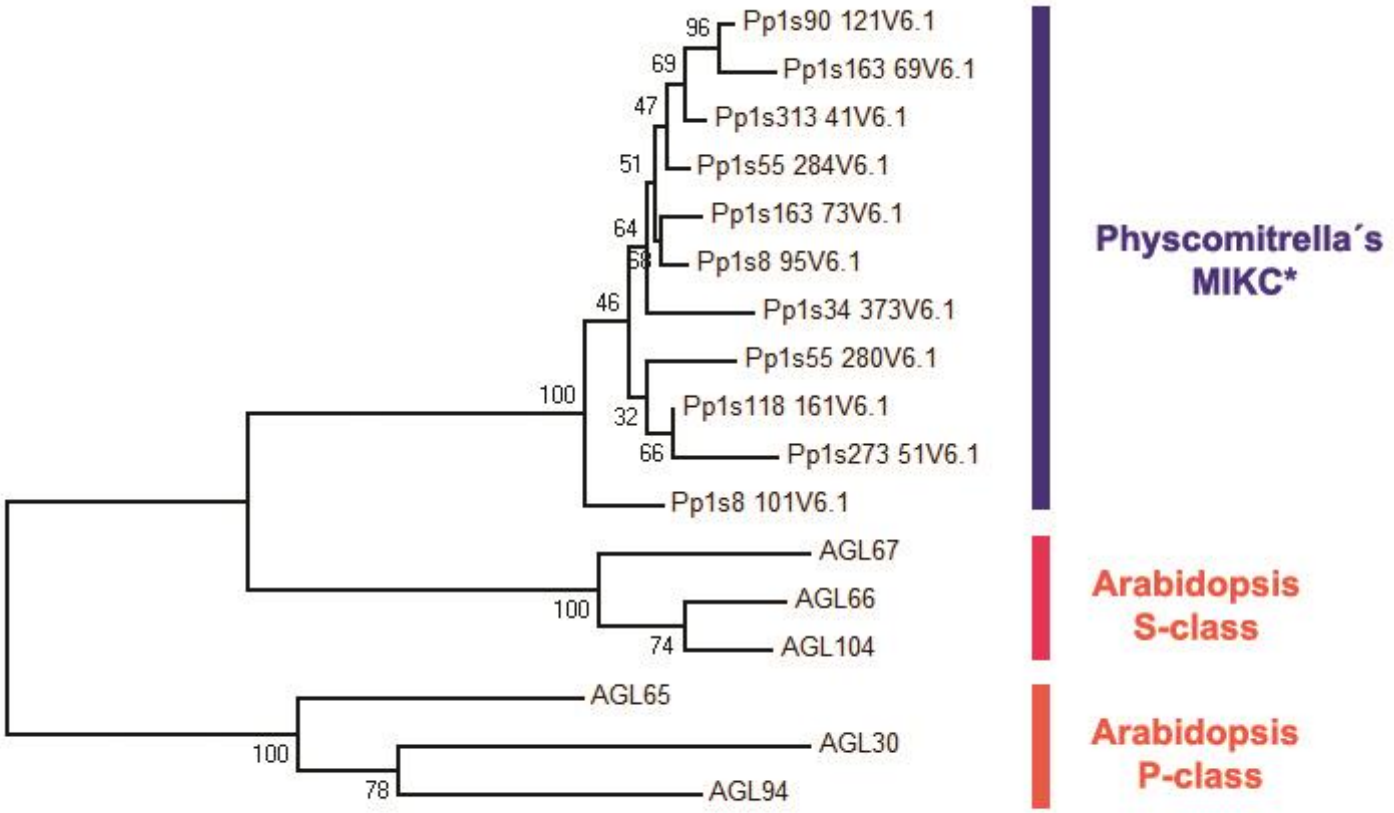

Supplemental Figure 5. Phylogenetic analysis of MIKC* genes. Phylogenetic tree constructed using maximum likelihood statistical method from aligned amino-acid sequences of MIKC* transcription factors from *Arabidopsis thaliana (AGL)* and *Physcomitrella patens (Pp).* Bootstrap support values are shown at the nodes of the tree.

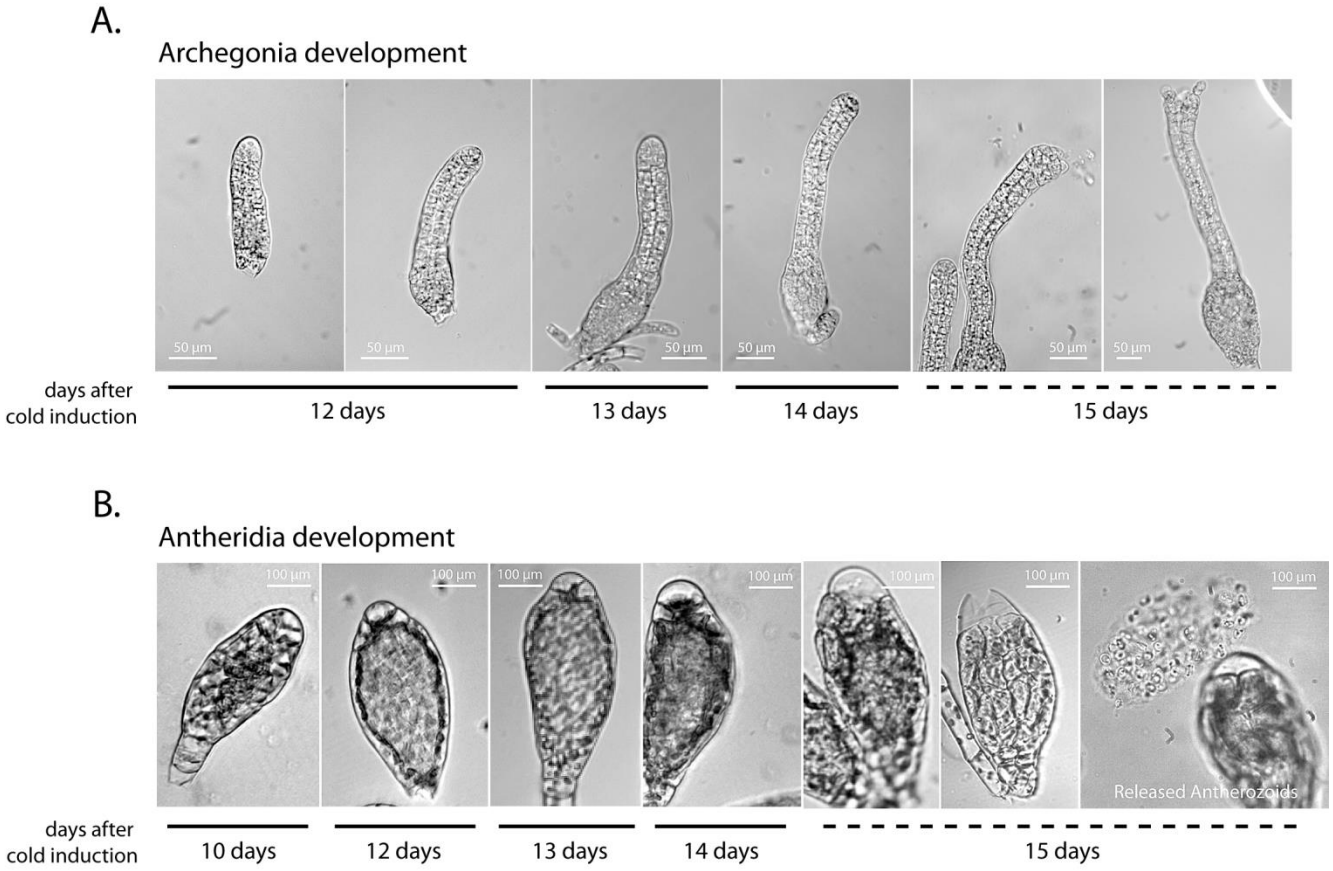

Supplemental Figure 6. Developmental characterization of gametangia. Induction of gametangia was conducted by exposing 3-4 week old gametophores to colder, short day conditions (17ºC, 8h light and 50% humidity). Observations were conducted almost every day after cold induction. (a) The developmental stages of archegonia from day 12 to 15 after cold induction are shown. At day 15 fully developed archegonia are observed. In many of them the channel leading to the egg cell appears open. (b) Antheridia development was followed in the same way. In this case, the most dramatic changes, besides growth, includes the change from green to yellow and the formation of a transparent “cap” at the anterior part of the organ. This cap brakes and the antherozoids are released. Sperm cell release events occur from day 14 and continue until day 17; however, it is during day 15 when we observed highest number of events. Both antheridia and archegonia can form organ clusters at different developmental stages. Reported dates represent the moment in which the depicted developmental stage was first seen.

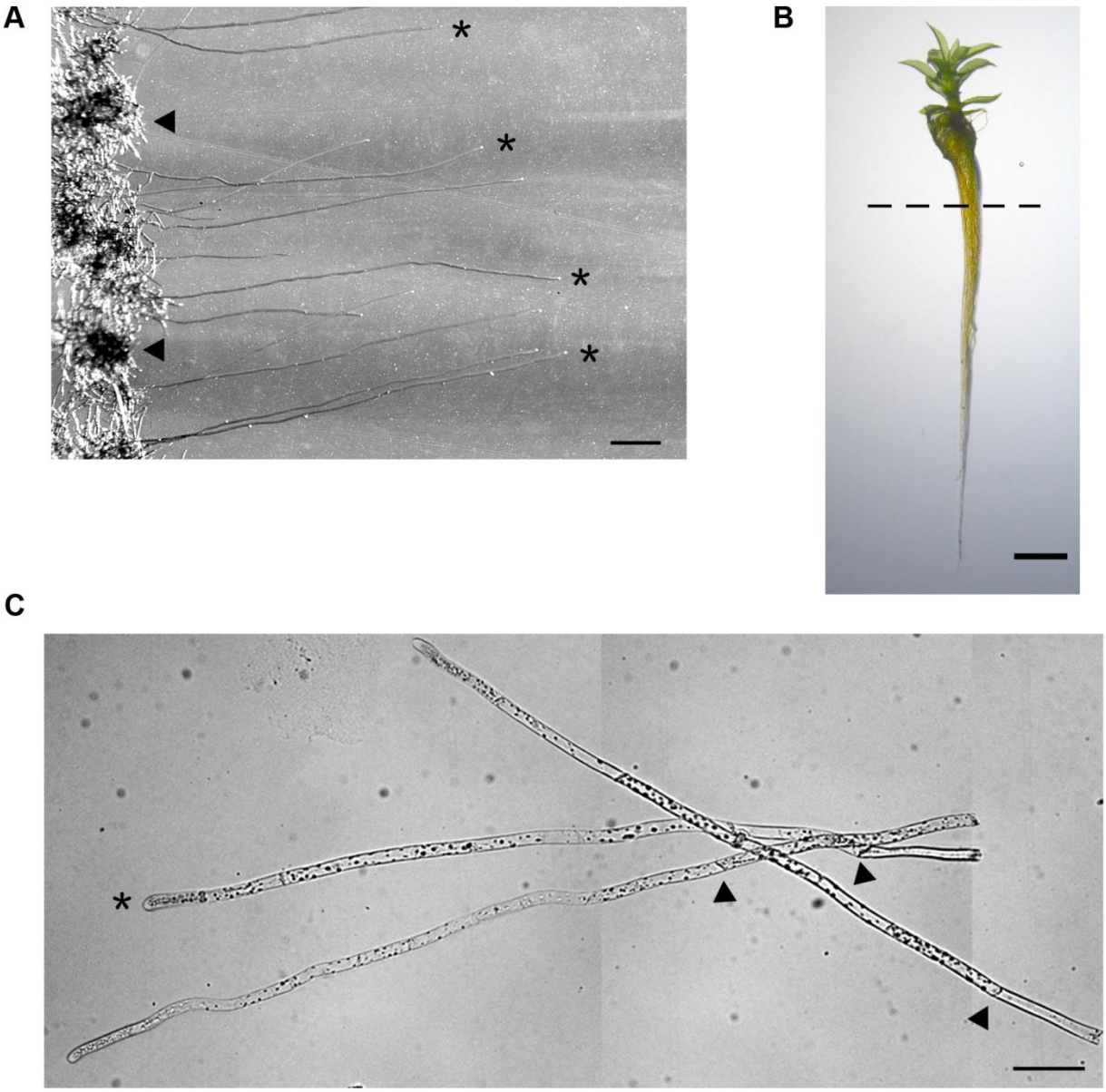

Supplemental Figure 7. Induction and isolation of caulonemal filaments and rhizoids. Caulonema was induced by exposing 4-5 day old protonema to dark conditions in KNOPS medium containing glucose and covered with cellophane (25ºC and 50% humidity) for 5 days. (a) Caulonemal filaments at the moment of isolation for RNA extraction (asterisks) 5 days after induction. At this stage they can be clearly distinguished and separated from the chloronemal filaments at the base (arrowhead). Scale bar = 300μM. (b) Representative gametophore with rhizoids at the moment of rhizoid dissection. Rhizoids were cut well below the base of the gametophores to avoid tissue contamination. Scale bar = 1.25 mm. (c) magnification of dissected caulonema showing the oblique cell plates (arrowheads) and clear tip region (asterisk) characteristic of caulonema. Scale bar = 50μM.

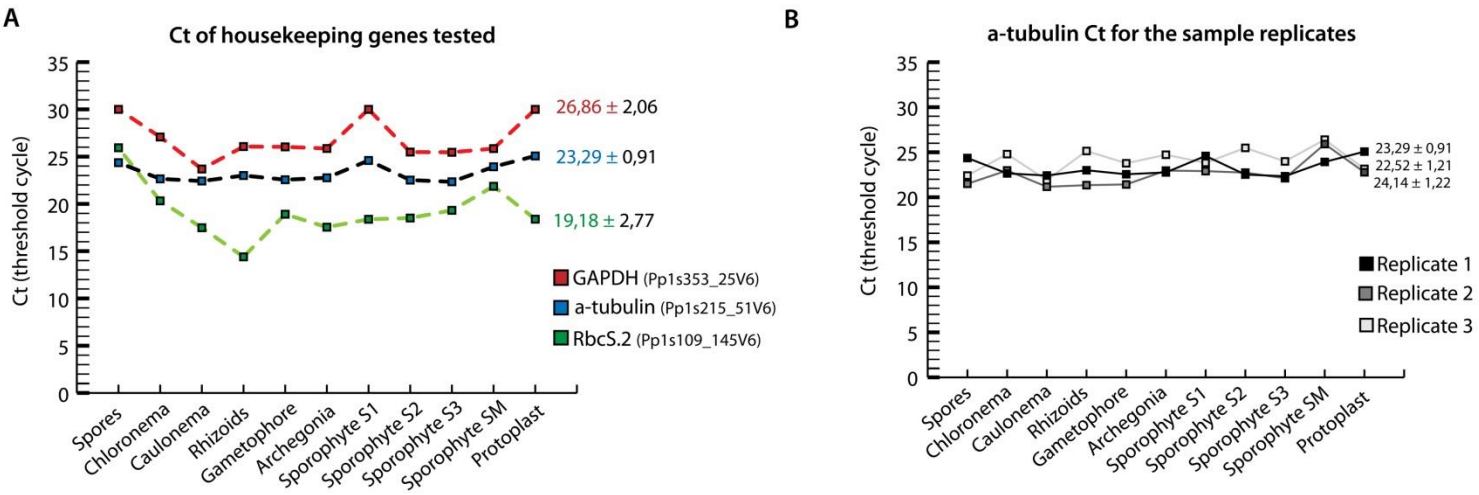

Supplemental Figure 8. Analysis of several reported housekeeping genes to determine consistency in gene expression across different samples. (a) Comparison among reported housekeeping genes Glyceraldehyde 3-phosphate dehydrogenase (GAPDH), alpha-tubulin (a-tubulin) and Rubisco chloroplast encoded subunit (RbcS.2) shows a more stable profile for alpha-tubulin. (b) Expression of the housekeeping gene alpha-tubulin was tested showing low variation among sample replicates and tissue samples.

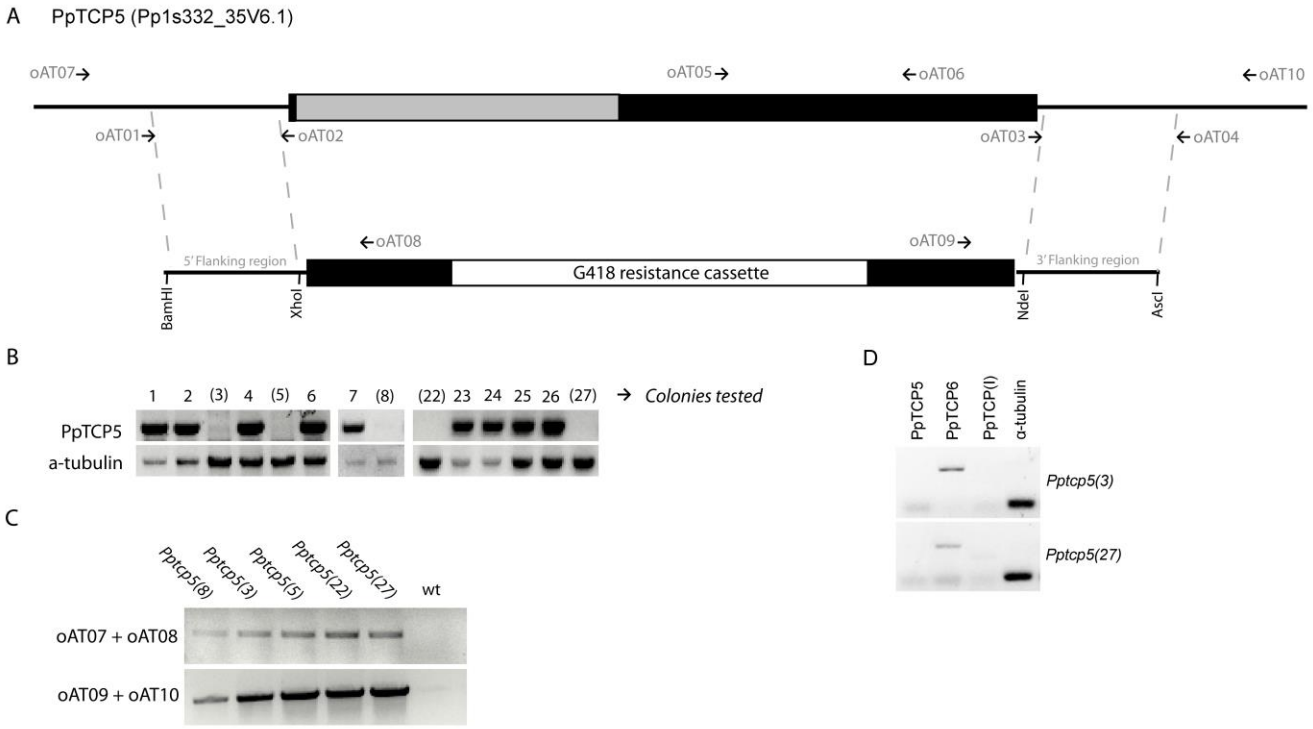

Supplemental Figure 9. Characterization of *Pptcp5* knockout plants. (a) Schematic representation of the construct used for PpTCP5 homologous recombination. The localization of the primers used for the cloning and characterization of the knockout *Pptcp5* lines are represented. (b) Genotyping of potentially positive *Pptcp5* knockout colonies after three rounds of G418 selection using primers oAT05 and oAT06. Lines 3,5,8,22 and 27 show a disruption of the WT locus. (c) Corroboration of the insertion points in the genome was performed by PCR using the indicated primers. The amplification for both 5' (oAT07 + oAT08) and 3' (oAT09 + oAT10) insertion points are shown for the five stable knockout lines identified. (d) Expression of TCP class II and class I (PpTCPI) genes in mutant lines Pptcp5(3) and Pptcp5(27) measured by RT-PCR.

Supplemental figure 1 references:

Finka, A., Saidi, Y., Goloubinoff, P., Neuhaus, J.M., Zryd, J.P., and Schaefer, D.G. (2008). The knock-out of ARP3a gene affects F-actin cytoskeleton organization altering cellular tip growth, morphology and development in the moss Physcomitrella patens. Cell Motil. Cytoskeleton 65: 769–784.

Goss, C.A., Brockmann D.J., Bushoven, J.T., Roberts, and A.W. (2012). A cellulose synthase (CESA) gene essential for gametophore morphogenesis in the moss Physcomitrella patens. Planta 235: 1355–1367.

Harries, P.A., Pan, A., and Quatrano, R.S. (2005). Actin-related protein2/3 complex component ARPC1 is required for proper cell morphogenesis and polarized cell growth in Physcomitrella patens. Plant Cell 17: 2327-2339.

Ishikawa, M., et al. (2011). Physcomitrella cyclin-dependent kinase A links cell cycle reactivation to other cellular changes during reprogramming of leaf cells. Plant Cell 23: 2924-2938.

Komatsu K., Suzuki N., Kuwamura M., Nishikawa Y., Nakatani M., Hitomi O., Takezawa D., Seki M., Tanaka M., Taji T., Hayashi T., and Sakata Y. (2012). Group A PP2Cs evolved in land plants as key regulators of intrinsic desiccation tolerance. Nature Comm. 4: 2219

Lavy, M., Prigge, M.J., Tigyi, K., and Estelle, M. (2012). The cyclo-philin DIAGEOTROPICA has a conserved role in auxin signaling. Development. 139: 1115–1124.

Liénard, D., Durambur, G., Kiefer-Meyer, M., Nogué, F., Menu-Bouaouiche, L., Charlot, F., Gomord, V., and Lassalles, P. (2008) Water transport by aquaporins in the extant plant Physcomitrella patens. Plant Physiology 146: 1207-1218.

Martin, A., Lang, D., Heckmann, J., Zimmer, A.D., Vervliet-Scheebaum, M., and Reski, R. (2009). A uniquely high number of *ftsZ* genes in the moss *Physcomitrella patens.* Plant Biol.11 (5): 744–750.

Noy-Malka C., Yaari R., Itzhaki R., Mosquna A., Gershovitz N.A., Katz A., and Ohad N. (2014). A single CMT methyltransferase homolog is involved in CHG DNA methylation and development of Physcomitrella patens. Plant Mol Biol. 84 (6): 719-735.

Perroud, P.F. and Quatrano, R.S. (2006). The role of ARPC4 in tip growth and alignment of the polar axis in filaments of Physcomitrella patens. Cell Motil. Cytoskeleton 63: 162-171.

Repp, A., Mikami, K., Mittmann, F., and Hartmann, E. (2004). Phosphoinositide-specific phospholipase C is involved in cytokinin and gravity responses in the moss Physcomitrella patens. Plant J. 40: 250–259.

Richter H., Lieberei R., Strnad M., Novák O., Gruz J., Rensing S.A., and Schwartzenberg K. (2012). Polyphenol oxidases in *Physcomitrella*: functional PPO1 knockout modulates cytokinin-dependent development in the moss *Physcomitrella patens.* J Exp Bot 63(14): 5121-35.

Saavedra, L., Balbi, V., Lerche, J., Mikami, K., Heilmann, I., and Sommarin. M. (2011). PIPKs are essential for rhizoid elongation and caulonemal cell development in the moss Physcomitrella patens. Plant J. 67: 635–647.

Sakakibara, K., Nishiyama, T., Deguchi, H., and Hasebe, M. (2008). Class 1 KNOX genes are not involved in shoot development in the moss Physcomitrella patens but do function in sporophyte development. Evolution & Development 10: 555–566.

Sakakibara K., Ando, S., Yip, H.K., Tamada, Y., Hiwatashi, Y., Murata, T., Deguchi, H., Hasebe, M., and Bowman, J.L. (2013). KNOX2 genes regulate the haploid-to-diploid morphological transition in land plants. Science. 339: 1067-1070.

Schipper, O., Schaefer, D., Reski R., and Flemin, A. (2002). Expansins in the bryophyte Physcomitrella patens. Plant Molecular Biology 50: 789–802.

Spinner, L., Pastuglia, M., Belcram, K., Pegoraro, M., Goussot, M., Bouchez, D., and Schaefer, D. G. (2010). The function of TONNEAU1 in moss reveals ancient mechanisms of division plane specification and cell elongation in land plants. Development 137: 2733–2742

Sugiyama, T., Ishida, T., Tabei, N., Shigyo, M., Konishi, M., Yoneyama, T., and Yanagisawa, S. (2012). Involvement of PpDof1 transcriptional repressor in the nutrient condition-dependent growth control of protonemal filaments in Physcomitrella patens. J. Exp. Bot. 63: 3185–3197.

Shu-Zon W., Ritchie J.A., Ai-Hong P., Quatrano R.S., and Bezanilla M. (2011). Myosin VIII regulates protonemal patterning and developmental timing in the moss Physcomitrella patens. Molecular Plant 4 (5): 909-921.

Vidali, L., Burkart G.M., Augustine R.C., Kerdavid E., Tüzel E., and Bezanilla M. (2010). Myosin XI is essential for tip growth in Physcomitrella patens. Plant Cell 22: 1868–1882.

Xu B., Ohtani M., Yamaguchi M., Toyooka K., Wakazaki M., Sato M., Kubo M., Nakano Y., Sano R., Hiwatashi Y., Murata T., Kurata T., Yoneda A., Kato K., Hasebe M., and Demura T. (2014). Contribution of NAC transcription factors to plant adaptation to land. Science 343: 1505-1508.